ISSN: 2633-4828 Vol. 6 No.1, January, 2024

International Journal of Applied Engineering & Technology

HIGH-FREQUENCY TRANSFORMER DESIGN FOR SOLID STATE TRANSFORMERS IN ELECTRIC POWER DISTRIBUTION SYSTEMS: A NOVEL DESIGN METHODOLOGY

Yam Krishna Poudel[1]*, Ramesh Kumar Pudasaini[2], Dashu Nath Kandel[3], Saroj Maharjan[4] and Yogesh Bhandari[5] and Jitesh Kumar Yadav[6]

[1]Assistant Professor, Department of Electrical and Electronics Engineering, Nepal Engineering College, Changunarayan, Bhaktapur Nepal,

[2]Assistant Professor, Department of Electronics and Communication Engineering, Nepal Engineering College, Changunarayan, Bhaktapur Nepal,

[3]Department of Electrical and Electronics Engineering, Nepal Engineering College, Changunarayan, Bhaktapur Nepal,

[4]Department of Electrical and Electronics Engineering, Nepal Engineering College, Changunarayan, Bhaktapur Nepal,

[5]Department of Electrical and Electronics Engineering, Nepal Engineering College, Changunarayan, Bhaktapur Nepal,

[6]Department of Electrical and Electronics engineering, School of engineering, Kathmandu University

[1]yampd01@gmail.com, [1]yamkp@nec.edu.np, [2]rameshkp@nec.edu.np, [2]pudasainiramesh29@gmail.com, [3]dashunath12@gmail.com, [4]sarojmaharjan@gmail.com, [5]bhandariyogesh360@gmail.com and [6]Jiteshky9860@gmail.com

ABSTRACT

This research paper presents a groundbreaking design methodology for high-frequency transformers, using power electronics devices named Solid-State Transformer (SST) used in distribution applications. SSTs have gained widespread popularity as an alternative to traditional 50/60 Hz transformers due to their exceptional power density, compatibility with distributed generation, DC grids, energy storage systems, and sensitive loads. Our proposed methodology takes into account the unique demands of SSTs such as active power flow control, harmonic suppression, voltage regulation, and reduced size and volume. The design process considers the influence of SST topologies on transformer design, including core and wire selections, isolation requirements, and different transformer structures. Our proposed design procedure has been implemented as an interactive tool in MATLAB® and ANSYS Software for designing high-frequency transformers with exceptional performance for SST applications in future energy systems with enhanced functionalities compared to traditional transformers. For validation A single phase 100KVA, 11KV/400V,3KHz SST is designed and calculate the total power loss, weight and efficiency at different frequencies. The results of our research clearly illustrate that Solid-State Transformers (SSTs) exhibit greater compatibility and significantly lower weight compared to traditional transformers operating at 50/60 Hz frequencies. These findings suggest that SSTs hold immense potential for use in future applications due to their enhanced compatibility and reduced weight, which are crucial factors in various industries such as renewable energy, transportation, and telecommunications. The lower weight of SSTs makes them more portable and easier to install, while their greater compatibility enables them to operate seamlessly with distributed generation systems, DC grids, energy storage systems, and sensitive loads. These advantages make SSTs an attractive alternative to traditional transformers, particularly in situations where weight and compatibility are critical considerations.

Keywords: Solid State Transformer (SST), Dual Active Bridge(DAB), Inverter, Rectifier

1. INTRODUCTION

A transformer is a device that harnesses electromagnetic induction to transfer energy. Its fundamental structure comprises two separate windings, the primary and secondary, and a magnetic core. The principles of Ampere's law and Faraday's law govern the functioning of transformers. These laws state that a current-generating conductor produces a surrounding magnetic field, and a voltage can be induced in a closed circuit due to the rate

of change in the magnetic flux (Shadfar et al., 2021a). Consequently, when an alternating current passes through the primary winding of the transformer, it generates a fluctuating magnetic field within the magnetic core, resulting in a voltage across the secondary winding. Traditional transformers operate at a line frequency of 50 Hz and can achieve remarkable efficiencies, often reaching up to 99% (Rehman & Ashraf, 2019) .Figure 1 shows the Generic Electric power System which consists of generation ,transmission and distribution network .

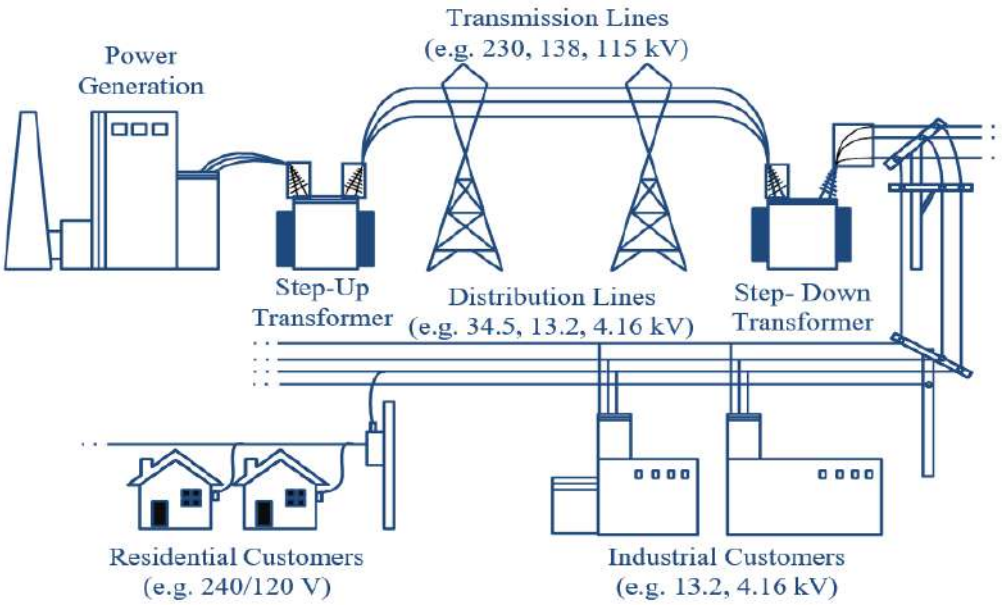

Figure 1: Generic Electric Power System

The conventional transformer is quite effective at what it does. However, in the future, energy systems will require features beyond just stepping up and down voltages, which the conventional 50Hz transformer cannot provide. Bidirectional power flow is provided by a modern electrical energy equipment called a solid state transformer (Zengin & Boztepe, 2014). It is also known as a power electronic transformer or smart transformer. With a high frequency transformer to step voltage up and down, it is composed of power electronic stages that are AC-DC, DC-DC, and DC-AC (Ortíz-Marín et al., 2024). There are three main components to it: a converter that creates high frequency AC from line frequency AC input, a high frequency transformer for isolation, and finally a converter that creates line frequency AC from high frequency AC (Chetri et al., n.d.). Here Figure 2 illustrate the modern power electronics based Solid State Transformer.

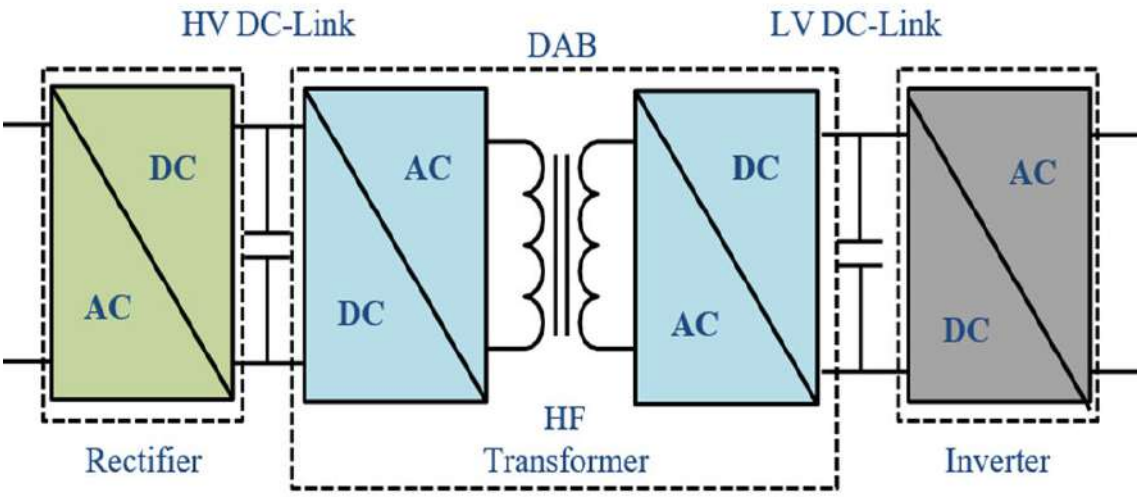

Figure 2: Solid State Transformer

It improves voltage regulation, harmonic isolation, power quality regulation, decoupling between high- and low-voltage networks, and power flow control. The input rectifier is served to convert AC-DC. It provides constant voltage and control the flow of current between the grid and DC-DC conversion stage (Singirikonda et al., 2022). Dual Active Bridge is a highly efficient isolated bidirectional DC-DC converter. It provides constant power with a better range at higher efficiency (Shadfar et al., 2021b). Figure 3 demonstrate Optimization between Volume, Cost and Efficiency.

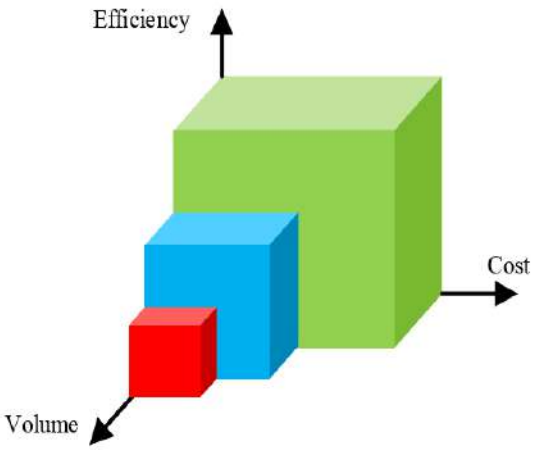

Figure 3: Optimization between Volume, Cost and Efficiency

2. LITERATURE REVIEW

The literature review on solid state transformers (SSTs) highlights their potential as an alternative solution for traditional electromechanical transformers in various applications due to their higher efficiency, smaller size, and faster response time. The review covers various aspects of SSTs, including design considerations, control strategies, and applications in power systems.

(Rehman & Ashraf, 2019) provide a comprehensive review of SSTs, covering their history, technology, construction, and applications in the distribution system. The authors discuss the advantages and challenges of SSTs, such as high switching frequency, high voltage stress, and harmonic distortion. They also review the different topologies and control strategies for SSTs, such as the dual active bridge (DAB) and the resonant converter.

(Zengin & Boztepe, 2014) propose a modified dual active bridge (MDAB) photovoltaic inverter for SST applications. The MDAB inverter has a higher efficiency and lower harmonic distortion compared to the traditional DAB inverter due to the use of a resonant tank circuit.

(Chetri et al., n.d.)present a study of various design approaches for SST implementation. The authors discuss the design considerations for the transformer, the rectifier, and the inverter, as well as the control strategies for SSTs. They also provide a comparison of the different design approaches based on their efficiency, cost, and complexity.

(Shadfar et al., 2021b)provide an overview of SSTs, discussing their concept, topology, and applications in the smart grid. The authors highlight the benefits of SSTs, such as their ability to provide reactive power, their compatibility with renewable energy sources, and their potential to reduce transmission losses.

(Aggeler et al., 2008) present a compact, high voltage, and high frequency DC-DC converter based on SiC JFETs for SST applications. The converter has a high efficiency, a high power density, and a low EMI level due to the use of SiC JFETs.

(Fan & Li, 2011) propose a high-frequency transformer isolated bidirectional DC-DC converter module for SST applications. The converter has a high efficiency over a wide load range, a high power density, and a low EMI level due to the use of a high-frequency transformer.

(An et al., 2019) present a simple power estimation with triple phase-shift control for the output parallel DAB DC-DC converters in power electronic traction transformer for railway locomotive application. The authors discuss the challenges of SSTs in railway applications, such as the high voltage stress and the high switching frequency, and propose a solution based on the use of triple phase-shift control.

(Ortiz et al., 2017) present the design and experimental testing of a resonant DC-DC converter for SST applications. The converter has a high efficiency, a high power density, and a low EMI level due to the use of a resonant tank circuit.

(Chen & Divan, 2017) discuss the design considerations of high voltage and high frequency three-phase transformers for SST applications. The authors highlight the challenges of SST transformers, such as the high voltage stress, the high switching frequency, and the harmonic distortion, and propose solutions based on the use of high-frequency transformers.

(Yun et al., 2018) present the implementation of a single-phase SST for the interface between a 13.2 kV MVAC network and a 750 V bipolar DC distribution. The authors discuss the challenges of SSTs in this application, such as the high voltage stress and the high switching frequency, and propose a solution based on the use of a single-phase SST.

(Ge et al., 2015) present energy feed-forward and direct feed-forward control strategies for SSTs. The authors discuss the advantages and disadvantages of these control strategies, such as their ability to improve the dynamic response and the stability of the SST, and propose a solution based on the use of energy feed-forward control.

(Garcia Rodriguez et al., 2017)propose a new SST topology comprising boost three-level AC/DC converters for applications in electric power distribution systems. The authors discuss the advantages and disadvantages of this topology, such as its ability to provide high voltage and high power density, and propose a solution based on the use of boost three-level converters.

(Leung et al., 2010) discuss the design considerations of high voltage and high frequency three-phase transformers for SST applications. The authors highlight the challenges of SST transformers, such as the high voltage stress, the high switching frequency, and the harmonic distortion, and propose solutions based on the use of high-frequency transformers.

(Rashidi et al., 2017) present the design and implementation of a series resonant SST. The authors discuss the advantages and disadvantages of this topology, such as its ability to provide high voltage and high power density, and propose a solution based on the use of a series resonant tank circuit.

(Lee et al., 2019) present the modeling and control of three-level boost rectifier based medium-voltage SSTs for DC fast charger applications. The authors discuss the challenges of SSTs in this application, such as the high voltage stress and the high switching frequency, and propose a solution based on the use of three-level boost rectifiers.

(Rehman et al., 2022) provide a comprehensive review of SSTs, covering their history, technology, construction, and applications in the distribution system. The authors discuss the advantages and challenges of SSTs, such as high switching frequency, high voltage stress, and harmonic distortion, and propose solutions based on the use of advanced control strategies and high-frequency transformers.

(Saleh et al., 2019) present a review of SSTs for distribution systems, covering their technology and construction. The authors discuss the advantages and challenges of SSTs, such as their ability to provide reactive power and their compatibility with renewable energy sources, and propose solutions based on the use of advanced control strategies and high-frequency transformers.

(Shafei et al., 2019) present a high power high frequency transformer design for SST applications. The authors discuss the challenges of SST transformers, such as the high voltage stress and the high switching frequency, and propose a solution based on the use of a high-frequency transformer.

(Shrestha et al., n.d.) present a model and analysis of SSTs. The authors discuss the advantages and disadvantages of SSTs, such as their ability to provide high efficiency and their compatibility with renewable energy sources, and propose a solution based on the use of advanced control strategies.

(Shao et al., 2022) present a review of dual active bridge (DAB) DC-DC converters for SST applications. The authors discuss the advantages and disadvantages of DAB converters, such as their ability to provide high efficiency and their compatibility with high voltage and high frequency applications, and propose solutions based on the use of advanced control strategies.

(Liu et al., 2019) present the design and implementation of a high efficiency control scheme for dual active bridge based 10 kV/1 MW solid state transformer for PV application. The authors discuss the challenges of SSTs in this application, such as the high voltage stress and the high switching frequency, and propose a solution based on the use of a dual active bridge converter.

(Yang et al., 2016) present a study of solid state transformers under imbalanced loads in distribution systems. The authors discuss the challenges of SSTs in this application, such as the impact of imbalanced loads on the performance and the stability of the SST, and propose solutions based on the use of advanced control strategies.

(Verma et al., 2018) present a review of SSTs for electrical systems, discussing their challenges and solutions. The authors highlight the benefits of SSTs, such as their ability to provide high efficiency and their compatibility with renewable energy sources, and propose solutions based on the use of advanced control strategies and high-frequency transformers.

(Xu She & Huang, 2013) present a review of SSTs in the future smart electrical system. The authors discuss the benefits and challenges of SSTs in this application, such as their ability to provide high efficiency and their compatibility with renewable energy sources, and propose solutions based on the use of advanced control strategies and high-frequency transformers.

(Krishnamoorthy & Yerra, 2018) present a review of solid state auto-transformer concepts for multi-pulse rectifiers. The authors discuss the advantages and disadvantages of this concept, such as its ability to provide high

efficiency and its compatibility with high voltage and high frequency applications, and propose solutions based on the use of advanced control strategies and high-frequency transformers.

In summary, the literature review highlights the potential of SSTs as an alternative solution for traditional electromechanical transformers in various applications due to their higher efficiency, smaller size, and faster response time (Khan et al., 2023). The review covers various aspects of SSTs, including design considerations, control strategies, and applications in power systems. The authors discuss the advantages and challenges of SSTs, such as high switching frequency, high voltage stress, and harmonic distortion, and propose solutions based on the use of advanced control strategies and high-frequency transformers (Xu et al., 2022). The review also highlights the benefits and challenges of SSTs in various applications, such as railway, PV, and smart grid applications. Overall, the review provides a comprehensive understanding of SSTs and their potential applications in power systems (Helali & Khedher, 2023).

3. RESEARCH METHODOLOGY

The different topologies are used in the practice are shown in figure 4.

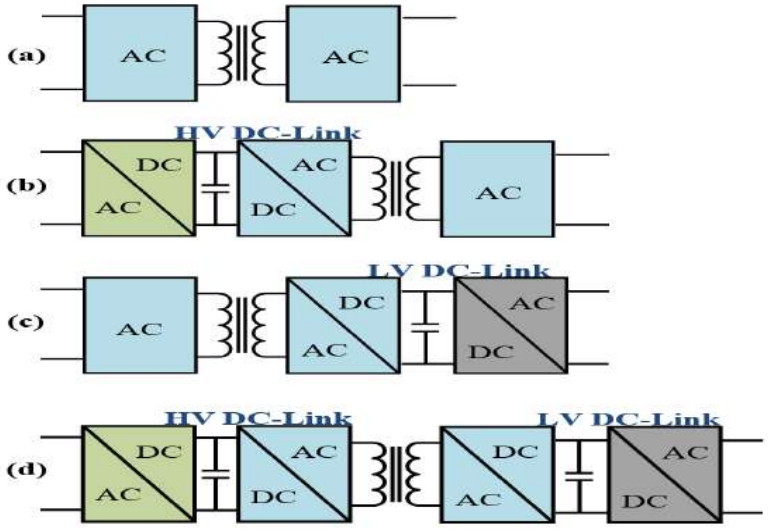

Figure 4: Different types of SST topologies

The model used in this research paper is shown in figure 5 below

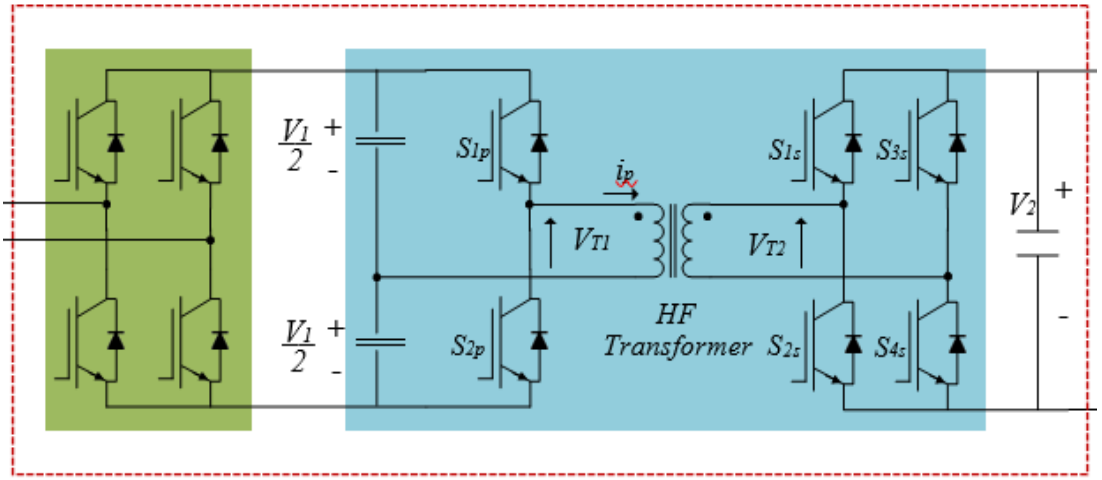

Figure 5: SST model used in research

$$C_{dc} = \frac{P_{rated}}{4 * F_{grid} * \left(V_{dc}^2 - (V_{dc} - V_{ripple})^2\right)}$$ …Equation (1)

Output DC voltage of Rectifier is calculated as

$$V_{dc} = \frac{2 * V_{max}}{\pi}$$ …Equation (2)

A power electronic circuitry known as an inverter is responsible for converting direct current (DC) into alternating current (AC). The AC frequency produced varies depending on the specific device utilized.

$$Inverter\ Rating = \frac{Total\ power}{Efficiency * power\ factor}$$ …Equation (3)

$$V_{dc} = \frac{3 * 2 * V_{max}}{\pi}$$ …Equation (4)

$$C = \frac{0.01 * s}{V^2 * 2\pi f}$$ …Equation (5)

3.1 Clark Park Transformation

A mathematical transformation known as the "ABC to DQ transformation" is applied in control theory and electrical engineering. It is mostly used to transform three-phase variables (A, B, and C) into two-phase variables (D and Q) in three-phase alternating current (AC) systems. Electric motors and generators, which are three-phase AC equipment, are frequently controlled by means of this transformation. The Park and Clarke transformations served as the foundation for this one. Let's dissect it in detail (O'Rourke et al., 2019):

Clarke Transformation (a, b, c to α, β):

The process of converting three-phase quantities (a, b, c) into two-phase stationary reference frame (α, β) values involves the use of the Clarke transformation. The system's phase A component is in line with the α-axis as shown in figure 6.

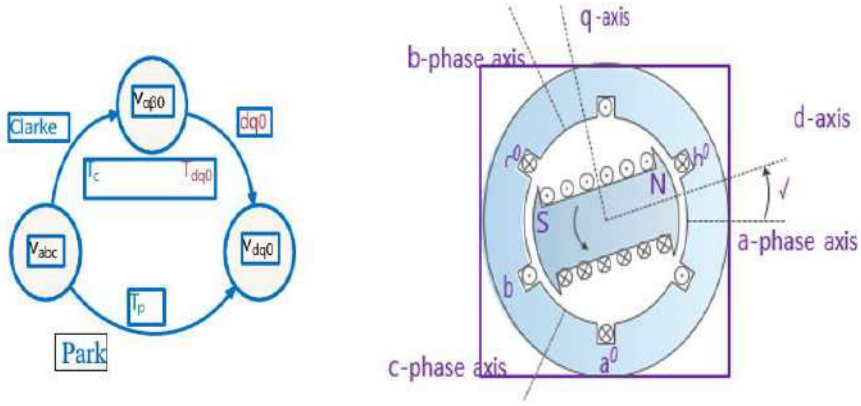

Figure 6: illustration of Clarke and park transformation

Park Transformation (α, β to D, Q):

The αβ reference frame is transformed into a rotating reference frame (DQ) that spins at the same frequency as the system's angular velocity (often the rotor speed in motor control applications) using the Park transformation, also called the dq transformation. The Q-axis is 90 degrees ahead of the D-axis, and the D-axis is parallel to the α-axis. We can transform the three-phase quantities (a, b, c) into the two-phase rotating reference frame (D, Q) by sequentially performing the Clarke and Park transformations. The control of AC machines and other applications requiring the decoupling and management of the machine's torque-producing current (Q-axis) and magnetic field (D-axis) will find this transformation to be especially helpful.

$$\begin{bmatrix} fa \\ fb \\ fc \end{bmatrix} = \begin{bmatrix} \cos(\alpha) & -\sin(\alpha) \\ \cos(\alpha-\beta) & -\sin(\alpha-\beta) \\ \cos(\alpha+\beta) & -\sin(\alpha+\beta) \end{bmatrix} * \begin{bmatrix} fd \\ fq \end{bmatrix} \quad \text{…Equation (6)}$$

This configuration consists of three stages. First, a back-end inverter (DC-AC) converts direct current (DC) to alternating current (AC). Next, a dual-active bridge (DAB) stage (DC-DC) with a high or medium frequency transformer manages input current control and high-voltage (HV) DC link. The rectifier step follows, enabling voltage regulation. The DAB stage facilitates power flow control, adjusts voltage levels, and manages the low-voltage (LV) DC link. The transformer's leakage inductance allows energy storage and transfer. Finally, the inverter stage converts the voltage back to 50 Hz for connecting AC loads.

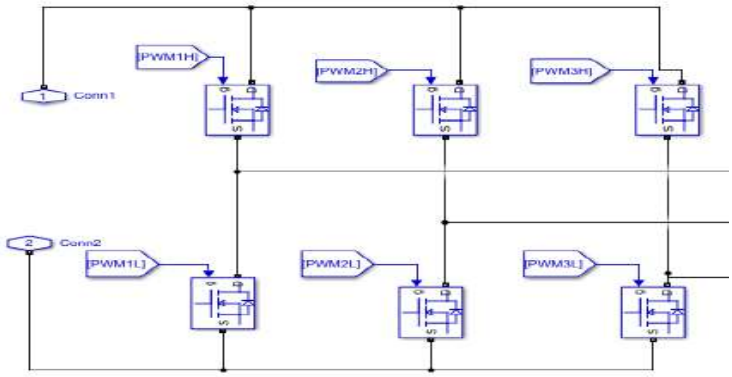

Figure 7: MATLAB model of thyristor configuration for Rectifier

Rectifier: Using the six thyristor switches, we first approximated a single rectifier. The purpose of the pulse generators installed in each switch was to provide rectangular pulses for the rectifier. Utilizing a set of thyristor, the rectifier transformed the AC input voltage into a pulsing DC voltage. The thyristor was placed so that it would flow current while rectifying the waveform. We utilized a filter together with other components because the pulsating voltage that resulted was not evenly distributed.

Dual Active Bridge:

Comparably, in the Dual Active Bridge simulation, four MOSFETs were employed in the high frequency transformer's primary side, and four thyristor were connected in the transformer's secondary side. Pulse generators were also supplied to the MOSFET and THYRISTOR. The input of DAB is a DC voltage that flows via a MOSFET and into a transformer. The transformer's output also comes from a thyristor, providing a step-down DC output voltage. Between two converters, the DC connection served as a buffer and guaranteed a steady DC voltage output. An inductor plus a sizable capacitor make up this device (Jeong et al., 2022). The energy transmitted from the first converter was retained by the capacitor and given to the second

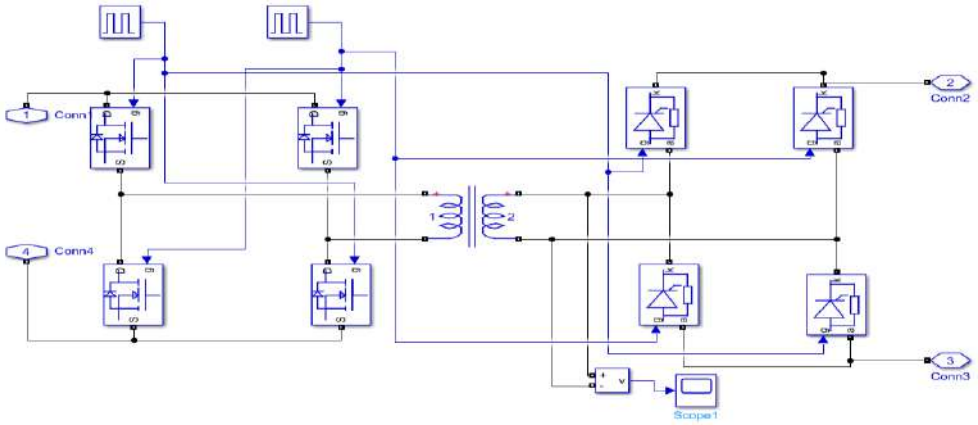

Figure 8: Dual Active Bridge

Conducting switches in the DAB is shown as below

$\theta < \theta \leq \delta$		$\delta < \theta \leq \phi$		$\phi < \theta \leq \pi$	
Bridge 1	**Bridge 2**	**Bridge 1**	**Bridge 2**	**Bridge 1**	**Bridge 2**
D1p D4p	D2s D3s	S1p S4p	S2s S3s	S1p S4p	D1s D4s

INVERTER:

Six MOSFETs were employed in the inverter to correct waves, and each MOSFET switch has a pulse generator. DAB output was used as the inverter's input, and it transformed it into the appropriate alternating voltage. The windings in a single phase transformer of the Shell type are grouped in a concentric pattern and encircled by a magnetic core. Laminated iron sheets are usually used for the magnetic core in order to minimize eddy current losses. This design makes the transformer more compact and efficient by giving the flux a shorter magnetic path and lowering the leakage flux.

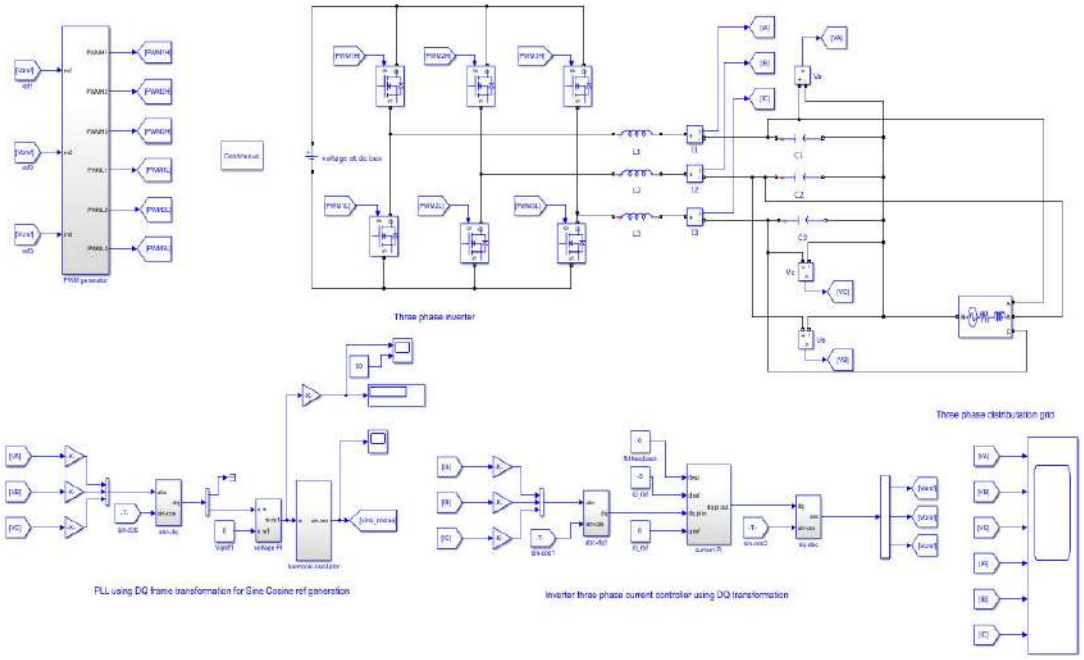

Figure 9: ABC to dq conversion

Shell Type Single Phase Transformer Figure 10 shown in below: For the transformer present in Dual Active Bridge, Design of Shell type single phase transformer was performed through ANSYS Electronics software. A single-phase shell-type transformer comprises three primary legs, structurally enhancing its core's mechanical robustness. Additionally, it strengthens the windings' defense against outside mechanical shocks. The center limb is wrapped in the HV and LV windings. The lateral limbs carry half of the flux (φ/2) while the central limb carries the complete flux (φ). As a result, the central limb's cross-section is twice that of the side limbs to accommodate the flux.

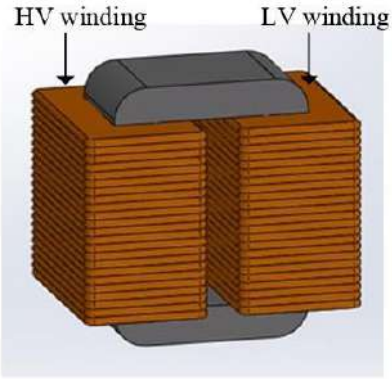

Figure 10: Shell Type Single Phase Transformer (2D)

4. RESULTS AND DISCUSSION

In this research, a Single-phase 100 kVA, 11 kV/400 V, 3 kHz solid-state transformer with continuous rating and natural cooling core type was designed. All calculations were done accordingly for distribution transformers in Table 1.

Result obtained this research are presented as bellows.

Table 1: Design consideration of 100KVA,11kv/400V,3KHz SST

Parameters	Value
Output	100 KVA
Voltage	V1/V2:11Kv/400V
Number of Phases	Single
Rating	Continuous
Cooling	Natural
Type	Core, Distribution

Max. Flux Density (Bm)	1Wb/m^2
Current Density (J)	3.5 A/mm^2
Factor K (in E=K√Q)	0.8
Window Space Factor	0.3
Core Stack Factor	0.95
Voltage Regulation	+5%

1. Design Calculation:

Table 2 presents the calculated parameters for the designed SST transformer. The net core area and gross core area were calculated as 6 m² and 6.315 m², respectively. The width and length of the window were set to 10 mm and 30 mm, respectively. The rectangular section of the transformer was determined to be 20 mm × 30 mm. The weight of iron was calculated as 0.646 kg, and the emf per turn was adjusted to 7.992 V after considering the core size. The secondary current, primary current, and lengths of the primary and secondary windings were also calculated. The cross-sectional areas of the primary and secondary conductors were determined as 2.473 mm² and 7.142 mm², respectively. The primary winding turns, secondary winding turns, central leg width, core stack height, input S1, overall width, and efficiency were also calculated.

2. Calculation for Rectifier & DAB:

Table 3 presents the calculation of parameters for the rectifier and DAB. The output DC voltage and capacitor values were determined as 9902 V and 0.2 F, respectively.

3. Calculation for Inverter:

Table 4 presents the calculation for the inverter. The rating, input DC voltage, capacitor, and inductor values were determined as 40 kW, 8002 V, 20 μF, and 25 mH, respectively. Overall, these calculations were performed based on the given parameters and design considerations. The results obtained from these calculations can be used to design and implement the SST, rectifier, and inverter components of the system.

Table 2: Parameters value used in research

Parameters	Values
Resistivity of copper (ρ) at 20 0 C	0.017 Ω-m
Density of iron	7.70 g/cc
Density of copper	8.93 g/cc
Specific iron loss	1 W/Kg

Table 3 shows design calculation. Table 4 shows calculation for Rectifier and DAB. Table 5 shows calculation for inverter.

Table 3: Calculated Parameters for Designed SST Transformer

Parameters	Values	Parameters	Values
Net core area Ai	6*10-4m2	Width of window Ww	10mm
Gross core area Agi	6.315*10-4m2	Length of window, Lw	30mm
Rectangular section	20 *30 mm	Weight of iron	0.646 kg
Emf per turn after core size adjusted	7.992 V	Iron loss	0.646 w
Secondary Current, I2	25 A	Length of mean turn, l_{mt}	0.1314m
Primary Current, I1	8.658 A	Length of Primary winding L1	180.93m
Cross Section Area of primary conductor A1	2.473mm2	Length of secondary winding L2	6.9642m
Cross Section Area of secondary conductor A2	7.142mm2	Weight of copper	4.43kg
Primary winding turns N1	1377	Copper loss Wc	104W

Secondary winding turns N2	53	Total loss	104.646 W
Central leg width Tw	20mm	Total Weight	5.186kg
Core stack height Hs	30mm	InputS1	100.083 KVA
Overall width W	60mm	Efficiency	99.9%

Table 4: Calculation of parameters of Rectifier & DAB

Output DC Voltage (V_{dc})	**Capacitor(C)**	**Capacitor(C)**
9902 V	0.2 F	0.2 F

Table 5: Calculation for Inverter

Rating (KW)	**Input DC Voltage (Vdc)**	**Capacitor(C)**	**Inductor(L)**
40	800 V	20 *10^-6 F	25* 10^-3 H

In summary, Figures 10, 11, and 12 illustrate the output characteristics of the rectifier, Dual Active Bridge, and Inverter components of the Solid-State Transformer system, respectively. Figure 10 shows that the rectifier output is 9902 V DC when a 11 kV AC input voltage is applied. This graph demonstrates that the rectifier successfully converts the AC input voltage into a DC output voltage. Similarly, Figure 11 displays the output voltage of the Dual Active Bridge, which is 800 V DC when a 9902 V DC input voltage is applied. This graph demonstrates the effectiveness of the Dual Active Bridge in converting DC input voltage into DC output voltage. Lastly, Figure 12 shows the output voltage of the Inverter, which is 400 V AC when an 800 V DC input voltage is applied. This graph demonstrates that the Inverter successfully converts DC input voltage into AC output voltage. These figures provide visual representations of the performance of each component in the Solid-State Transformer system.

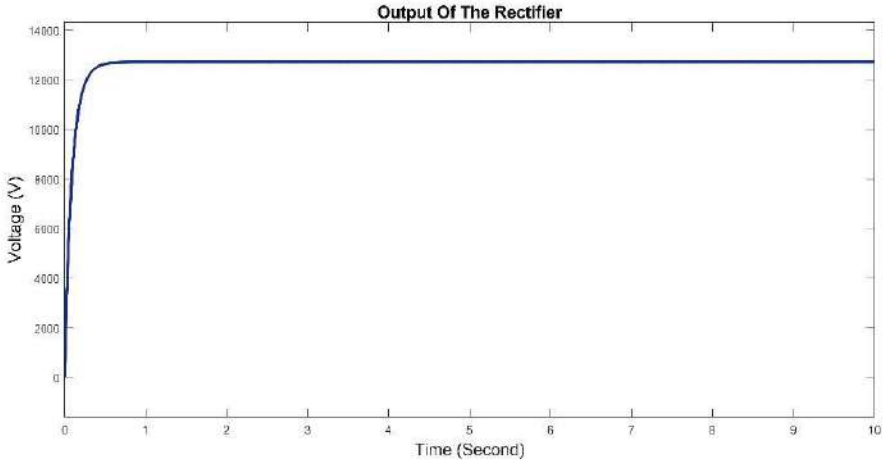

Figure 10: output of the rectifier

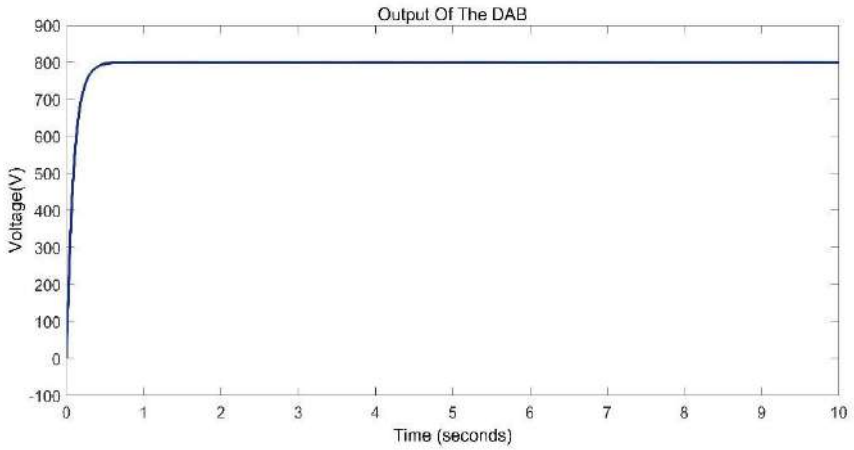

Figure 11: Output of the DAB Bridge

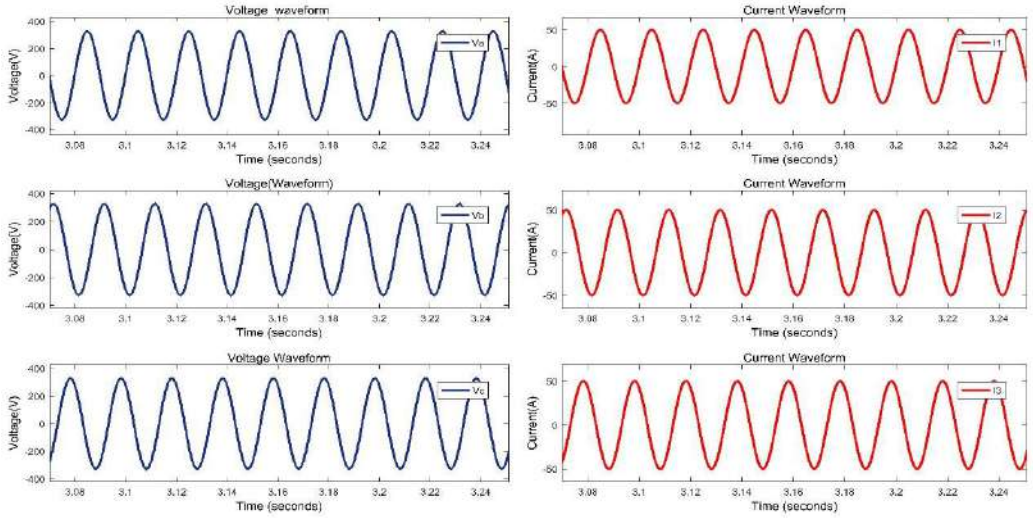

Figure 12: End output of the SST for Phase power (V_{rms})

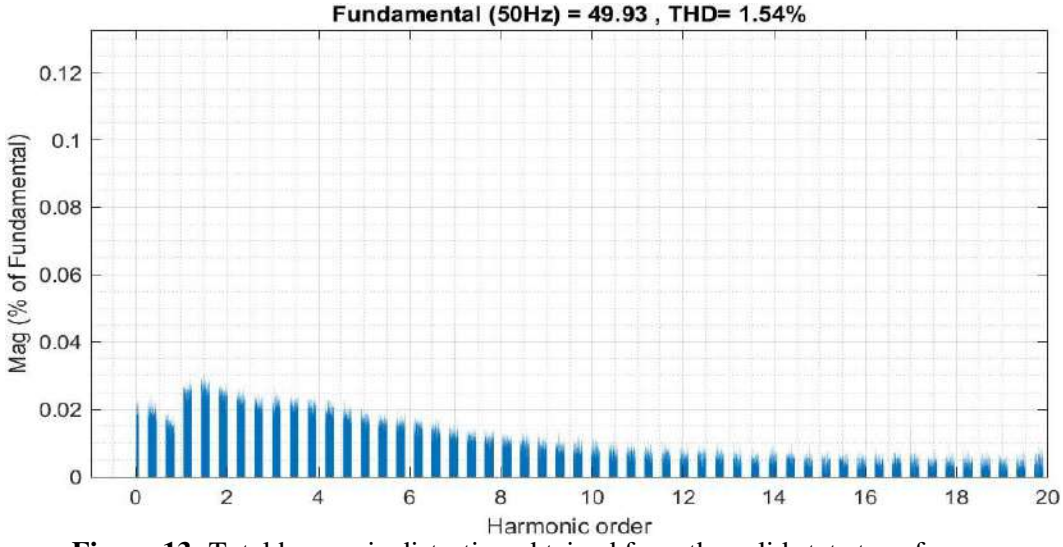

Figure 13: Total harmonic distortion obtained from the solid state transformer

In this experiment, the total harmonic distortion (THD) in the output waveform of a solid-state transformer was measured at 1.54% as shown in Figure 13. According to IEEE standards, THD should be below 3% for acceptable power quality. Since the measured value falls within this range, the power quality from the solid-state transformer design is considered satisfactory.

Table 6: Comparison of impact of high frequency on weight of Iron, weight of copper and total weight of the transformer

Frequency	Weight of Iron (Kg)	Weight of Copper (Kg)	Total Weight (Kg)	Efficiency
50 Hz	412.78	34.48	448	99 %
500 Hz	4.088	10.73	14.91	99.79%
1kHz	3.973	7.893	11.912	99.85%
3kHz	0.646	4.43	5.186	99.9%
10 kHz	0.075	2.66	2.83	99.95%

From the aforementioned table 6, it is evident that as the frequency increases, the iron weight drastically decreases, and the copper weight reduces significantly as well. Consequently, the overall weight of the transformer is reduced. For a conventional 50 Hz transformer, the iron weight amounts to 412.78 kg, and the copper weight is 34.48 kg, resulting in a total transformer weight of 448 kg with an efficiency of 99%. In contrast, for the modern SST with a 3 kHz frequency employed in solid-state transformers, the iron weight is only 0.646 kg, and the copper weight is 4.13 kg, totaling 5.186 kg with a remarkable efficiency of 99.9%.

5. CONCLUSION

In conclusion, this study has successfully demonstrated the feasibility of developing circuits for individual rectifiers, dual active bridges, and inverters, which can be combined to create a whole solid-state transformer using MATLAB & ANSYS electronics. Here inverter circuit was managed via the ABC-to-DQ Control algorithm, which allowed us to produce a 220V AC output from an 800V DC input using an inverter fed by a high-frequency step-down transformer. The ABC-to-DQ transformation technique was also applied to manage three-phase AC systems mathematically during this study. Through this research work we have gained insights into the weight reduction potential of transformers at high frequencies while also observing an increase in efficiency through MATLAB & ANSYS electronics simulations. However, there are some limitations to this study that need to be addressed in future research directions such as improving the efficiency of the solid-state transformer at low frequencies by implementing advanced control strategies or exploring new materials for semiconductor devices to reduce power losses during switching operations at high frequencies. Additionally, further research is required to investigate the feasibility of integrating multiple phases into a single solid-state transformer to reduce the overall size and weight of the transformer while maintaining high efficiency levels at various frequencies.

CONFLICTS OF INTEREST

The authors state unequivocally that they have no conflicts of interest with this study.

REFERENCES

Aggeler, D., Biela, J., & Kolar, J. W. (2008). A compact, high voltage 25 kW, 50 kHz DC-DC converter based on SiC JFETs. *2008 Twenty-Third Annual IEEE Applied Power Electronics Conference and Exposition*, 801–807. https://doi.org/10.1109/APEC.2008.4522813

An, F., Song, W., Yang, K., Yang, S., & Ma, L. (2019). A Simple Power Estimation With Triple Phase-Shift Control for the Output Parallel DAB DC–DC Converters in Power Electronic Traction Transformer for Railway Locomotive Application. *IEEE Transactions on Transportation Electrification*, *5*(1), 299–310. https://doi.org/10.1109/TTE.2018.2876057

Chen, H., & Divan, D. (2017). High-frequency transformer design for the soft-switching solid state transformer (S4T). *2017 IEEE Applied Power Electronics Conference and Exposition (APEC)*, 2534–2541. https://doi.org/10.1109/APEC.2017.7931054

Chetri, C., Boruah, M., Borah, N. N., & Devi, P. (n.d.). Study of Various Design for SST Implementation. *International Journal of Scientific Research and Engineering Development*, *3*.

Fan, H., & Li, H. (2011). High-Frequency Transformer Isolated Bidirectional DC–DC Converter Modules With High Efficiency Over Wide Load Range for 20 kVA Solid-State Transformer. *IEEE Transactions on Power Electronics*, *26*(12), 3599–3608. https://doi.org/10.1109/TPEL.2011.2160652

Garcia Rodriguez, L. A., Jones, V., Oliva, A. R., Escobar-Mejia, A., & Balda, J. C. (2017). A New SST Topology Comprising Boost Three-Level AC/DC Converters for Applications in Electric Power Distribution Systems. *IEEE Journal of Emerging and Selected Topics in Power Electronics*, *5*(2), 735–746. https://doi.org/10.1109/JESTPE.2017.2677523

Ge, J., Zhao, Z., Yuan, L., & Lu, T. (2015). Energy Feed-Forward and Direct Feed-Forward Control for Solid-State Transformer. *IEEE Transactions on Power Electronics*, *30*(8), 4042–4047. https://doi.org/10.1109/TPEL.2014.2382613

Helali, H., & Khedher, A. (2023). Performance study of control strategies applied to smart transformer model based on a five-level cascaded H-bridge rectifier. *Computers and Electrical Engineering*, *110*, 108864. https://doi.org/10.1016/j.compeleceng.2023.108864

Jeong, D.-K., Yun, H.-J., Park, S.-H., Kim, M.-H., Ryu, M.-H., Baek, J.-W., & Kim, H.-S. (2022). 13.2 kV Class 3-Phase Solid State Transformer System Based on EtherCAT Communication. *Electronics*, *11*(19), 3092. https://doi.org/10.3390/electronics11193092

Khan, W., Dar, J. A., Parihar, K. S., & Pathak, M. K. (2023). Analysis of a New Single-Stage AC/AC Converter for Solid-State Transformer. *IEEE Transactions on Industry Applications*, 1–13. https://doi.org/10.1109/TIA.2023.3343312

Krishnamoorthy, H. S., & Yerra, S. (2018). Solid state auto-transformer concept for multi-pulse rectifiers. *2018 IEEE Applied Power Electronics Conference and Exposition (APEC)*, 2362–2367. https://doi.org/10.1109/APEC.2018.8341346

Lee, M., Yeh, C.-S., Yu, O., Kim, J.-W., Choe, J.-M., & Lai, J.-S. (2019). Modeling and Control of Three-Level Boost Rectifier Based Medium-Voltage Solid-State Transformer for DC Fast Charger Application. *IEEE Transactions on Transportation Electrification*, *5*(4), 890–902. https://doi.org/10.1109/TTE.2019.2919200

Leung, C., Dutta, S., Baek, S., & Bhattacharya, S. (2010). Design considerations of high voltage and high frequency three phase transformer for Solid State Transformer application. *2010 IEEE Energy Conversion Congress and Exposition*, 1551–1558. https://doi.org/10.1109/ECCE.2010.5618234

Liu, T., Yang, X., Chen, W., Li, Y., Xuan, Y., Huang, L., & Hao, X. (2019). Design and Implementation of High Efficiency Control Scheme of Dual Active Bridge Based 10 kV/1 MW Solid State Transformer for PV Application. *IEEE Transactions on Power Electronics*, *34*(5), 4223–4238. https://doi.org/10.1109/TPEL.2018.2864657

O'Rourke, C. J., Qasim, M. M., Overlin, M. R., & Kirtley, J. L. (2019). A Geometric Interpretation of Reference Frames and Transformations: dq0, Clarke, and Park. *IEEE Transactions on Energy Conversion*, *34*(4), 2070–2083. https://doi.org/10.1109/TEC.2019.2941175

Ortíz-Marín, J., Ruiz-Robles, D., Moreno-Goytia, E. L., & Venegas-Rebollar, V. (2024). Design and implementation of a Central-Tapped Medium Frequency Transformer with nanocrystalline core for high-

efficiency DC-DC SAB converters. *Electric Power Systems Research*, *227*, 109900. https://doi.org/10.1016/j.epsr.2023.109900

Ortiz, G., Leibl, M. G., Huber, J. E., & Kolar, J. W. (2017). Design and Experimental Testing of a Resonant DC–DC Converter for Solid-State Transformers. *IEEE Transactions on Power Electronics*, *32*(10), 7534–7542. https://doi.org/10.1109/TPEL.2016.2637827

Rashidi, M., Sabbah, M., Bani-Ahmed, A., Nasiri, A., & Balali, M. H. (2017). Design and implementation of a series resonant solid state transformer. *2017 IEEE Energy Conversion Congress and Exposition (ECCE)*, 1282–1287. https://doi.org/10.1109/ECCE.2017.8095937

Rehman, A., & Ashraf, M. (2019). Design and Analysis of PWM Inverter for 100KVA Solid State Transformer in a Distribution System. *IEEE Access*, *7*, 140152–140168. https://doi.org/10.1109/ACCESS.2019.2942422

Rehman, A., Imran-Daud, M., Haider, S. K., Rehman, A. U., Shafiq, M., & Eldin, E. T. (2022). Comprehensive Review of Solid State Transformers in the Distribution System: From High Voltage Power Components to the Field Application. *Symmetry*, *14*(10), 2027. https://doi.org/10.3390/sym14102027

Saleh, S. A. M., Richard, C., St. Onge, X. F., McDonald, K. M., Ozkop, E., Chang, L., & Alsayid, B. (2019). Solid-State Transformers for Distribution Systems–Part I: Technology and Construction. *IEEE Transactions on Industry Applications*, *55*(5), 4524–4535. https://doi.org/10.1109/TIA.2019.2923163

Shadfar, H., Ghorbani Pashakolaei, M., & Akbari Foroud, A. (2021a). Solid-state transformers: An overview of the concept, topology, and its applications in the smart grid. *International Transactions on Electrical Energy Systems*, *31*(9). https://doi.org/10.1002/2050-7038.12996

Shadfar, H., Ghorbani Pashakolaei, M., & Akbari Foroud, A. (2021b). Solid-state transformers: An overview of the concept, topology, and its applications in the smart grid. *International Transactions on Electrical Energy Systems*, *31*(9). https://doi.org/10.1002/2050-7038.12996

Shafei, A. El, Ozdemir, S., Altin, N., Jean-Pierre, G., & Nasiri, A. (2019). A High Power High Frequency Transformer Design for Solid State Transformer Applications. *2019 8th International Conference on Renewable Energy Research and Applications (ICRERA)*, 904–909. https://doi.org/10.1109/ICRERA47325.2019.8996515

Shao, S., Chen, L., Shan, Z., Gao, F., Chen, H., Sha, D., & Dragičević, T. (2022). Modeling and Advanced Control of Dual-Active-Bridge DC–DC Converters: A Review. *IEEE Transactions on Power Electronics*, *37*(2), 1524–1547. https://doi.org/10.1109/TPEL.2021.3108157

Shrestha, S., Kc, M., & Tamrakar, I. (n.d.). *Modeling and Analysis of Solid State Transformer*.

Singirikonda, S., Obulesu, Y. P., Kannan, R., Reddy, K. J., Kiran Kumar, G., Alhakami, W., Baz, A., & Alhakami, H. (2022). Adaptive control-based Isolated bi-directional converter for G2V& V2G charging with integration of the renewable energy source. *Energy Reports*, *8*, 11416–11428. https://doi.org/10.1016/j.egyr.2022.08.223

Verma, N., Singh, N., & Yadav, S. (2018). Solid State Transformer for Electrical System: Challenges and Solution. *2018 2nd International Conference on Electronics, Materials Engineering & Nano-Technology (IEMENTech)*, 1–5. https://doi.org/10.1109/IEMENTECH.2018.8465315

Xu She, & Huang, A. (2013). Solid state transformer in the future smart electrical system. *2013 IEEE Power & Energy Society General Meeting*, 1–5. https://doi.org/10.1109/PESMG.2013.6672768

Xu, W., Huang, P., Liu, Z., Zhao, M., Dian, R., Wang, P., Wang, Q., Wang, D., & Shen, T. (2022). Analysis of temperature field of medium frequency transformer based on improved thermal network method. *IET Generation, Transmission & Distribution*, *16*(12), 2346–2356. https://doi.org/10.1049/gtd2.12451

Yang, T., Meere, R., O'Loughlin, C., & O'Donnell, T. (2016). Performance of solid state transformers under imbalanced loads in distribution systems. *2016 IEEE Applied Power Electronics Conference and Exposition (APEC)*, 2629–2636. https://doi.org/10.1109/APEC.2016.7468235

Yun, H.-J., Jeong, D.-K., Kim, H.-S., Kim, M., Baek, J.-W., Kim, J.-Y., & Kim, H.-J. (2018). Implementation of a Single-Phase SST for the Interface between a 13.2 kV MVAC Network and a 750 V Bipolar DC Distribution. *Electronics*, *7*(5), 62. https://doi.org/10.3390/electronics7050062

Zengin, S., & Boztepe, M. (2014). Modified dual active bridge photovoltaic inverter for solid state transformer applications. *2014 International Symposium on Fundamentals of Electrical Engineering (ISFEE)*, 1–4. https://doi.org/10.1109/ISFEE.2014.7050613

APPENDICES:

Design Calculation:

EMF per turn, $Et=K\sqrt{Q} = 0.8\sqrt{100}$

$= 8$

F=3Khz

Also, $E_t = 4.44\ B_m\ f\ A_i$

$\therefore$ Net core area, $A_i = 6*10^{-4}cm^2$

Gross core area, $Agi= Ai /Ks= 6.315*10^{-4}m^2$

$\therefore$ Use a core of either square section of size $\sqrt{631.5} = 25.12mm^2$

(Or) rectangular section of size 20*30 mm as available in market

Here, a rectangular core is preferred for construction.

$\therefore$ Adjusted core size is $A_i = 20*30= 600mm^2$

New $E_t= 7.992V$

Secondary current, $I_2= 100$ KVA/ 400V= 25 A

Primary current, $I_1= 100KVA/11KV*1.05 = 8.658$ A (5% extra for losses)

Cross section area of primary conductor, $A_1 = I_1/J = 2.473mm^2$

Dia. of primary conductor, $d_1 = \sqrt{(4/\pi)} *2.473 = 1.774$ mm (bare) = 1.774+ 0.01 = 1.784mm (with enamel insulation)

Cross section area of secondary conductor, $A_2 = I_2/J = 7.142mm^2$

Dia. of secondary conductor, $d2 = \sqrt{(4/\pi)}*7.142 = 3.015$mm (bare) = 3.015 + 0.01 =3.0255mm (with enamel insulation)

Primary winding turns, $N_1=V_1/E_t=1377$

Secondary winding turns, $N_2= (V_2/E_t) *1.05 =53$ (5% extra for voltage drop)

Core dimensions:

Central leg width, $T_w=20mm$

Core stack height, $H_s=30mm$

Width of 'I' section=Tw/2= 10mm

Overall width, W = 3*Tw= 60mm

Length of 'E' section, L = 5* Tw/2 = 50mm

Width of window, Ww= Tw/2 = 10mm

Length of window, $L_w = 1.5*T_w$ = 30mm

Core stamping selected = 0.50mm

No. of clamping's required = Hs/ (thickness of each lamination) =60mm

No. of E's required = 40 and I's =20

Weight of iron = total – 2windows = [(6*5*3)-2(1*3)] *7.7 = 0.646Kg

∴ Iron loss = 0.646*1 = 0.646w

Window Arrangement:

Length of mean turn, Lmt = 2(Tw+Hs) + π h (where h=height of winding=Tw/2)

=0.1314m

Length of primary winding, L1= N1*Lmt

=18093.78cm

Length of secondary winding, L2 = N2*Lmt

=696.42cm

Weight of copper = volume of copper * specific copper density

=4.43 Kg (considering lead connection to pri & sec)

Resistance of primary winding, $R_1 = \rho l / a_1$

= 1.243Ω

Resistance of secondary winding, $R_2 = \rho l / a_2$

= 0.0165 Ω

Voltage drop (sec.) = I_2*R_2

= 0.4125 V

Copper loss, $W_c = I_1^2 *R_1 + I_2^2 *R_2$

= 104 W

Total loss = copper loss + iron loss

=104.646 W

Total weight = iron weight + copper weight + misc. like insulation, clamps

= 646.8+ 4439.97+ 100

= 5.186 Kg

Input (S1) = output (S2) + losses

= 100.083KVA

Apparent efficiency, η = S2/S1 *100

= 99.9%

For Rectifier

$$C_{dc} = \frac{P_{rated}}{4 * F_{grid} * \left(V_{dc}^2 - \left(V_{dc} - V_{ripple}\right)^2\right)}$$

Take ripple voltage =0.4 V

$$C_{dc} = \frac{100 * 10^3}{3} \frac{1}{4 * 50\left((1267^2) - (1267 - 0.4)^2\right)}$$

=0.2 F

Output dc voltage of Rectifier

$$V_{dc} = \frac{2 * V_{max}}{\pi}$$

$$V_{max} = 1.414 * V$$

$$V_{dc} = \frac{2 * 1.414 * 11000}{\pi}$$

=9902 V dc

For Dual Active Bridge

$$C_{dc} = \frac{P_{rated}}{4 * F_{grid} * \left(V_{dc}^2 - \left(V_{dc} - V_{ripple}\right)^2\right)}$$

$$C_{dc} = \frac{100 * 10^3}{3} \frac{1}{4 * 50\left((800^2) - (800 - 0.5)^2\right)}$$

=0.2F

For Inverter

Rating of Inverter

Take total power =25000

Power factor =0.8

Efficiency = 80%=0.8

$$Inverter\ Rating = \frac{Total\ power}{Efficiency * power\ factor}$$

$$= \frac{25000}{0.8*0.8}$$

=39062.5 VA

Choose 40 KVA or 40 KW Inverter

Switching frequency(fsw)=3KHz

Selection of resonant frequency

fres=$\frac{f_{sw}}{10} = \frac{3*10^3}{10}$=300Hz

Finding the value of capacitance

Reactive power =1%of rated power (s)

$$Q = \frac{v^2}{x_c} = V^2 \frac{(2\pi fc)}{1}$$

$$c = \frac{0.01 * s}{V^2 * 2\pi f}$$

Specification :100KV;230 Vp-p ,50 Hz

$$c = \frac{0.01 * (100 * 10^3)}{3 * 230^2 * 2\pi * 50}$$

$$c = 20 * 10^{-6}\ F$$

Finding the value of inductances

$$W_{res} = \frac{1}{\sqrt{c}Lp}$$

$$L = \frac{1}{w_{(sw)} \frac{I_{g(sw)}}{V_{i(sw)}} \left(1 - \frac{w_{sw}^2}{w_{re}^2}\right)}$$

$$current\ I_g = \frac{100}{3 * 230} * 1000$$

=144.92 A

Fsw=3KHz

Fres=300Hz

Ig(sw)=0.3% of Ig

=0.003*144.92

=0.434 A

Vi(sw)=0.9 times Vg

Vi(sw)=0.9*230=207 v

$$L = \frac{1}{2\pi * 3000 \left(\frac{0.434}{207}\right) \left(1 - \left(\frac{(2\pi * 3000)^2}{(2\pi * 300)^2}\right)\right)}$$

=25mH

Input dc voltage of inverter

$$V_{dc} = \frac{3 * 2 * V_{max}}{\pi}$$

$$V_{dc} = \frac{3 * 2 * 400}{\pi}$$

=764 V dc

≅800 V dc